We are IntechOpen, the world's leading publisher of Open Access books Built by scientists, for scientists

4,800
Open access books available

122,000
International authors and editors

135M
Downloads

Our authors are among the

154
Countries delivered to

TOP 1%
most cited scientists

12.2%
Contributors from top 500 universities

CLARIVATE ANALYTICS BOOK CITATION INDEX INDEXED

WEB OF SCIENCE™

Selection of our books indexed in the Book Citation Index in Web of Science™ Core Collection (BKCI)

Interested in publishing with us?
Contact book.department@intechopen.com

Numbers displayed above are based on latest data collected.
For more information visit www.intechopen.com

2

Glass-Ceramics Containing Nano-Crystallites of Oxide Semiconductor

Hirokazu Masai*, Yoshihiro Takahashi and Takumi Fujiwara
Tohoku University
**present affiliation: Kyoto University*
Japan

1. Introduction

1.1 Glass and Crystal

Inorganic glass materials generally possess high transparency, good formability, and tuneable chemical composition range. Since glass has no grain boundary, which is a characteristic of liquid, attained high transparency of glass makes it to be a fundamental material for our daily life, for examples, window, display panel glass and optical glass fibres. The good formability is originated from the random network structure with interstitial free volume, and therefore, large and long glassy material can be prepared much easier than inorganic crystal. Note that the term "random" in glass means a lack of the long-range ordering. Actually in glass there is a short-range ordering of atoms that constitute various coordination polyhedra. Thus, the short-range ordering in amorphous is basically identical to that in crystal. On the other hand, the random network of glass closely correlates with the chemical composition diversity, which in turn allows us to tailor physical property and various functionalities. The diversity is also a unique characteristic of amorphous glass materials.

The most conventional definition of glass is "an amorphous material possessing the glass transition behaviour". Figure 1 shows a typical volume change of glass and crystal as a function of temperature. In the case of crystal, transition from liquid to solidified crystal occurs at the melting temperature, T_m. On the other hand, a glass material takes the supercooled state below the T_m, and shows the transition to glass in the temperature range where the viscosity of glass increases to 10^{13} dPa·s. Temperature at which transition from supercooled liquid to glass occurs is mentioned as the glass transition temperature, T_g. In the temperature region, some physical parameters of glass material show "some steep" change. Since the T_g is a fictive temperature that depends on the fabrication process, a glass can take several values of T_g depending on the cooling rate. As shown in Fig. 1, there is a volume difference between crystal and the glass, which originates from the free volume of glass material possessing the random network. Because of the random network structure, the Gibbs free energy of a glass material is inherently larger than that of the corresponding crystal, and glass materials exist as a metastable state. It means that phase transition of glass to crystalline phase can progress above the T_g, at which migration of the compositional units

starts. The thermal transition process from glass to the corresponding crystal is called crystallization of glass. On the other hand, the resulted glassy material containing some precipitated crystallites is designated as a "glass-ceramic". Since the short-range ordering of glass is basically identical to that of crystal, the glass-ceramic can be said as a glassy material possessing partially long-range and/or medium-range ordering. Such glassy material containing both ordered and disordered parts is the main target of this chapter.

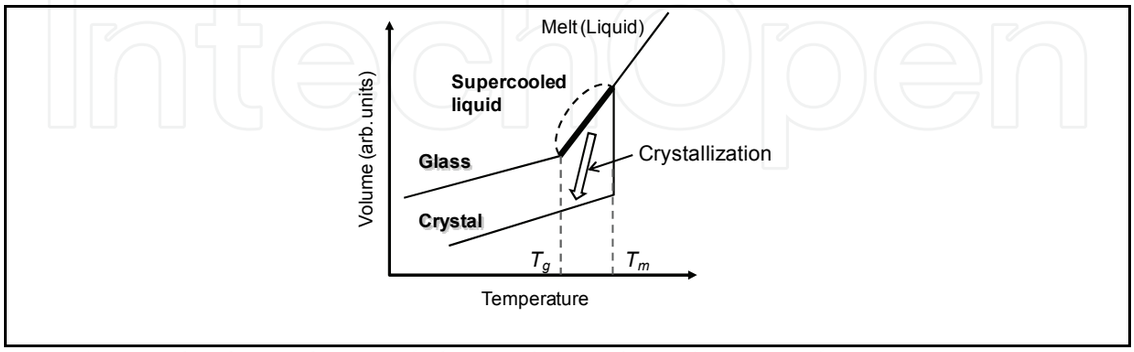

Fig. 1. A typical volume change of glass and crystal as a function of temperature.

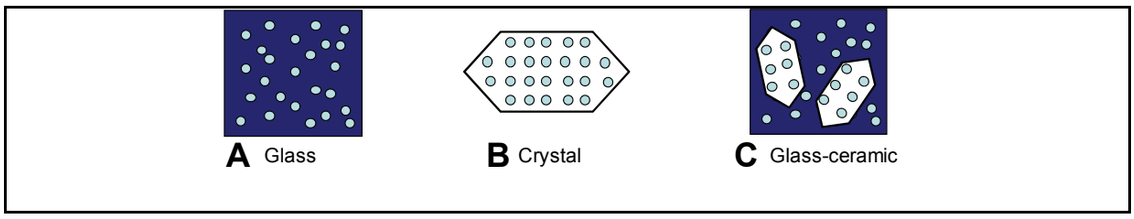

Fig. 2. Schematic images of (A) glass, (B) crystal, and (C) glass-ceramic.

1.2 Crystallization of Glass & Glass-Ceramic

It is natural that thermodynamically metastable amorphous glass changes into stable ordered crystal above the T_g. In earlier years, crystallization of glass was called devitrification of glass, because there is a difference in refractive index between the precipitated crystallites and the residual amorphous regions. The formation of boundary within a matrix by crystallization often brings about a loss of transparency of the material due to the Mie scattering. To overcome this problem, two approaches can be used: (I) tuning the refractive index by addition of various kinds of oxides, and (II) controlling the size of precipitated crystallites. The former approach is realized by using a database of optical property of glass matrix. Since the additivity between property and compositions usually holds in glass material, tailoring of refractive index can be attained empirically. On the other hand, the later approach is of importance even in a glass possessing the same chemical composition as the crystal, in that case the mismatch of refractive index between crystallites and residual amorphous is relatively small. Crystallization from a supercooled liquid state above the T_g progresses via two processes; i.e. nucleation and crystal growth. The rates of nucleation and crystal growth depend on the heat-treatment temperature as well as crystalline composition. Figure 3 shows a schematic depiction of rates of nucleation and crystal growth in glass. Although the details of these two processes are not mentioned here (please see some treatises, for examples, McMillan, 1979 or Strnad, 1986), an important point

is that nucleation and crystal growth can be independently controlled by careful heat-treatment procedure. As shown in Fig. 3, the maximum rates of nucleation and crystal growth occur at different temperatures. In addition, nucleation preferentially occurs in the low-temperature region above the T_g. Precipitation of either large crystallites (> several μm) or small crystallites (< several nm) is effective for maintaining the transparency of the glass after crystallization. The latter crystallization, in which nano-sized crystallites are precipitated, is often referred to as "nano-crystallization". In the case of precipitation of crystallites from the glass matrix that possesses chemical composition different from the stoichiometric composition of crystal, the nano-crystallization process is quite of importance. Glass-ceramic, which is usually obtained by heat-treatment, *i.e.* crystallization, of a precursor glass, is a kind of glassy material consisting of disordered glass regions and ordered precipitated crystalline regions. Since glass-ceramic permanently shows both glassy and crystalline characteristics without any temporal change below the T_g, it may be mentioned that glass-ceramic is an inorganic composite material possessing not only merits of glass materials but also its unique physical properties of the corresponding crystals. Conventional glass-ceramic is superior to the precursor glass in terms of strength, heat-resistance, and thermal shock resistance, because the nano-crystallites precipitated in the glass matrix. In addition, a combination of the physical properties of glass and crystal gives rise to novel functions. For example, commercially available low expansion glasses consist of both crystallites with negative thermal expansion and the residual amorphous parts that possess positive one. For obtaining desired glass-ceramic, control of the crystallization behaviour is needed as mentioned above. Indeed, several crystalline phases are sometimes simultaneously created from the same mother glass, and thus, the thermodynamic and kinetic control is necessary for obtaining the glass-ceramic with practical functions. However, in another respect, such diversity is the origin of various functionalities even in a glass-ceramic possessing the simple nominal chemical composition. A variety of properties of glass-ceramic, therefore, have motivated many researchers to fabricate novel functional devices (Beall & Pinckney, 1999, Takahashi et al., 2001, 2004, Masai et al., 2006).

In the chapter, the authors have described our recent works on fabrication of oxide semiconductor-containing transparent glass-ceramics. Such glass-ceramics will be a functional composite using the unique property of precipitated crystal. In addition, it is expected that physical property of precipitated crystallites in glass-ceramic is different from that of single crystal, because there is interface, which affects both the structure and physical property, between these materials. In the following sections, examination of correlation between chemical composition of glass and the precipitated crystal has been reported.

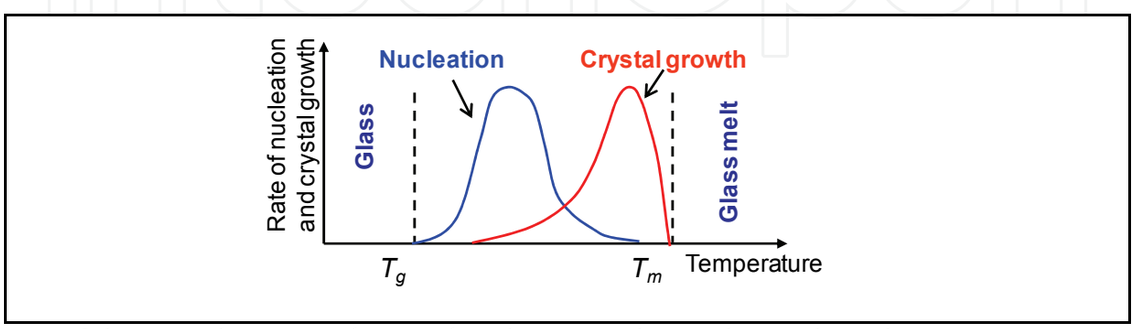

Fig. 3. Schematic depiction of rates of nucleation and crystal growth in glass.

2. Glass-Ceramics Containing TiO_2 Nano-Crystallites

2.1 Background

Titanium dioxide, TiO_2, has attractive characteristics, such as chemical stability, high refractive index, and it is used in electronic devices or as a photocatalyst. In particular, the photocatalysis of TiO_2 is industrially applied in many fields owing to its strong oxidation capability and high hydrophilicity (Fujishima & Honda, 1972). TiO_2-containing transparent materials are usually prepared by vapour deposition (Yeung & Lam, 1983), sputtering deposition, or by coating using a TiO_2-containing sol. However, the properties of TiO_2 produced by these deposition or coating techniques change over time by surface damage and thus a re-coating process of the material is necessary. In other words, there is the limitation of permanent performance in the TiO_2 deposition or coating materials. On the contrary, if the TiO_2 crystallites exist in the glass matrix, the TiO_2 crystallites dispersed in the glass matrix will exhibit a stable characteristic property even with surface polishing.

However, literature on crystallization of glass containing TiO_2 crystallites by a heat-treatment is scarce. Although studies of phase-separated TiO_2 glass have been reported, the obtained bulk glass is usually heterogeneous with a mixture of TiO_2 crystallites and other crystallites (Hosono et al., 1990). Indeed, it is extremely difficult to obtain selective crystallization of TiO_2, because a TiO_2 crystal acts as a nucleus of other crystalline phases and also because it forms another crystal structure with other glass forming oxides, such as Al_2O_3 or SiO_2 (as mentioned in 1.2). For example, there is a patent about the glass-ceramic containing TiO_2, in which rutile is crystallized by a heat-treatment (Brydges & Smith, 1976). Although it reported that the obtained glass-ceramics, which contained fibrous crystals of rutile, presented improvements of mechanical strength compared with the original mother glass, it also reported that additional crystallites $Al_4B_2O_9$ was coincidentally crystallized. In addition, it is difficult to attain a high degree of transparency in a TiO_2-crystallite-containing transparent glass, because of light scattering by TiO_2 crystallites with a large refractive index.

We can propose TiO_2 glass-ceramic as a promising material for several applications. First application is as a photocatalytic transparent material in which precipitated TiO_2 crystallites will play permanent photocatalytic property because of the fully dispersion. Second application is use in an optical element as a lasing optical device (Lawandy et al., 1994). The TiO_2 nano-crystallites in the glass matrix can confine light, which is suitable and interesting for random lasing, because the refractive index of TiO_2 is 2.52 (anatase) ~ 2.728 (rutile). Ling et al. demonstrated laser oscillation in a polymer film containing TiO_2 particles and an organic dye (Ling et al., 2001). If the host matrix of random media is an inorganic material, which has advantage in terms of durability better than organic material, it will break though the wall for the practical application of random lasing devices. On the other hand, if periodic nano-structure of TiO_2 can be fabricated, such material will be a photonic crystal that can control the lightwave. Since TiO_2-precipitated glass-ceramic can be a hybrid material such as solar sell (O'Regan, B. & Gratzel, 1991), there is wide diversity of the matrix using the unique physical property.

As a matter of fact, we have accidentally discovered the TiO_2-precipitated glass-ceramic. Different from a target Aurivillius $CaBi_4Ti_4O_{15}$ (Kato et al., 2004), unexpected TiO_2 crystalline phase was observed in the glass-ceramics in 2006. In other words, the present study was delivered by serendipity. The fact that such unexpected crystalline phase shows

the unique physical property in glass-ceramics is also an interesting point of study on glass-ceramics.

2.2 CaO-B_2O_3-Bi_2O_3-Al_2O_3-TiO_2 (CaBBAT) Glass

At an early stage, we investigated a glass forming region of the precursor glass using CaO-B_2O_3-Bi_2O_3-Al_2O_3-TiO_2 (CaBBAT) system. The molar ratio of CaO : Bi_2O_3 : TiO_2 was fixed at 1 : 2 : 4, which was a nominal stoichiometric composition ratio of $CaBi_4Ti_4O_{15}$, whereas that of B_2O_3, which belongs to network forming oxide group, was changed to obtain homogeneous transparent precursor glass. Glass samples were prepared by conventional melt-quenching method using alumina crucibles, and the eluted amount of Al_2O_3 from the crucible was estimated to be about 20 mol% using a fluorescence X-ray analysis. Table 1 shows the chemical compositions of the CaBBAT precursor glasses and their apparent transparencies. No homogenous precursor glass was obtained with the amount of B_2O_3 lower than 50 mol% (**1**, **2**, and **3**). On the other hand, we also found that about 10 mol% of Bi_2O_3 and 5 mol% of CaO were needed to prepare transparent precursor glasses (**7** and **8**). Note that only rutile crystallites were precipitated in all opaque precursor glasses after melt-quenching (Fig. 4). Therefore, it suggests that crystallization of rutile easily occurs in the glass system, and that quasi phase separation occurs during the crystallization process. Although the prepared $5CaO$-$65B_2O_3$-$10Bi_2O_3$-$20TiO_2$ glass melted in a platinum crucible was opaque because of crystallization of rutile TiO_2, the crystallization was prevented by addition of Al_2O_3 as a starting material. It indicates that Al_2O_3 was also essential for the transparency and homogeneity of the glass.

	Chemical composition (mol%)				Apparent	T_g (°C)	Precipitated
No.	CaO	Bi_2O_3	B_2O_3	TiO_2	transparency		crystalline phase
1	12.5	25	12.5	50	Opaque	–	Rutile
2	10	20	30	40	Translucent	–	Rutile
3	7	14	51	28	Translucent	–	Rutile
4	5	10	65	20	Transparent	569	–
5	5	10	75	10	Transparent	572	–
6	5	10	85	0	Transparent	510	–
7	5	5	70	20	Opaque	–	Rutile
8	0	10	70	20	Opaque	–	Rutile

Table 1. Several CaO-Bi_2O_3-B_2O_3-Al_2O_3-TiO_2 (CaBBAT) precursor glasses prepared using alumina crucible: Each value of T_g was measured using differential thermal analysis.

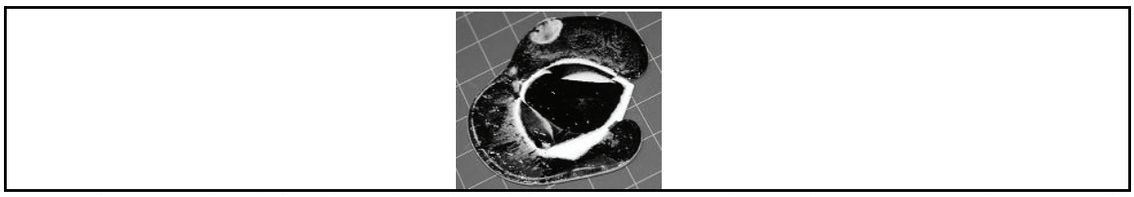

Fig. 4. Photograph of the CaBBAT glass (**3**). Rutile was selectively precipitated even in the precursor glass prepared by melt-quenching method.

The T_gs of TiO_2-containing transparent glasses were almost 570°C whereas TiO_2-free glass was 510°C. The result shows that T_g of the TiO_2-containing glass is dominated by local structure that correlates with titanium species. The obtained transparent precursor glasses were vinous in colour, and there was an absorption band around 490 nm (see Figs. 6A or 8B). These absorption bands are attributed to Bi-radical-like species or Bi_2 clusters (Khonthon et al., 2007, Murata & Mouri, 2007, Masai et al., 2009). Since shift of the absorption band in the visible region was observed by changing chemical composition, it is suggested that a structure consisting of several atoms affects formation of such Bi species.
Using the nominal composition of B_2O_3, we have called the CaBBAT glasses (**4**), (**5**), and (**6**) as CaBBAT65, CaBBAT75, and CaBBA85, respectively. Figure 5 depicts XRD patterns of the CaBBAT65, CaBBAT75, and CaBBA85 glass-ceramics heat-treated at 630°C for 3 h. Here, we have distinguished several samples by using an abbreviation, $\mathbf{C}_x$: a glass-ceramic with the heat-treatment temperature at x°C for 3 h. Compared the obtained patterns to the JCPDS pattern of rutile (JCPDS No. 01-084-1283), it is found that rutile was selectively precipitated in these glass-ceramics. Until 2007, there was no report on the selective crystallization of TiO_2 from glass matrix after heat-treatment. The obtained XRD patterns show the characteristic of the glass-ceramics.

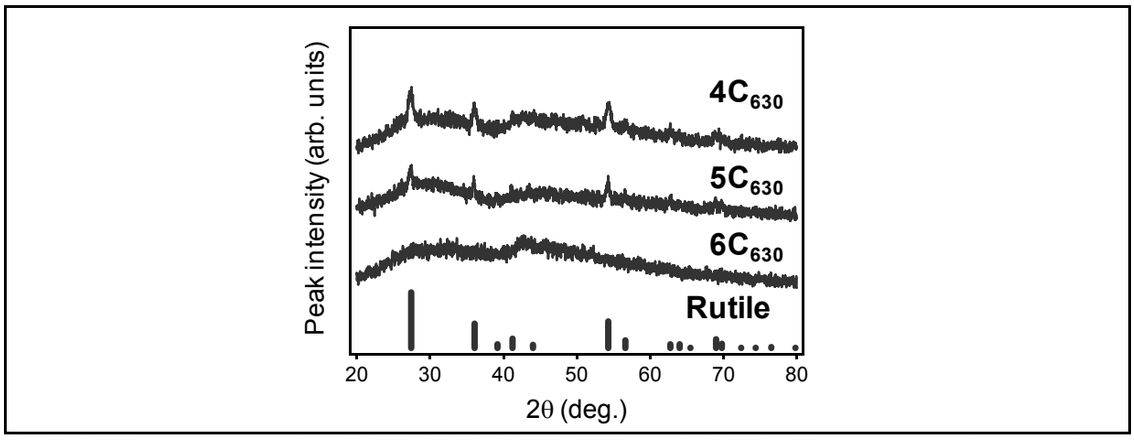

Fig. 5. XRD patterns of the CaBBAT65, CaBBAT75, and CaBBA85 glass-ceramics after heat-treatment at 630°C for 3 h: $\mathbf{4C}_{630}$, $\mathbf{5C}_{630}$, and $\mathbf{6C}_{630}$, respectively.

Figure 6A shows the absorption spectra of the CaBBAT65 glass (**4**), and the glass-ceramics ($\mathbf{4C}_{620}$, $\mathbf{4C}_{630}$, and $\mathbf{4C}_{640}$). The absorption coefficient increases with increasing heat-treatment temperature in the whole wavelength range covered. The apparent colour of the sample drastically changes after the heat-treatment above 625°C from transparent vinous to translucent blue. Figure 6B shows the photograph of the precursor glass (**4**) and the glass-ceramics ($\mathbf{4C}_{620}$ and $\mathbf{4C}_{640}$) whose thickness was about 500 μm. The colour of glass-ceramics depends on the heat-treatment temperature. On the other hand, Fig. 6C shows the photograph of the same samples with a white lighting from the backside. We can observe Chinese characters through these obtained glasses with backside lighting. Since the transmitted light is observable through these crystallized samples, it is suggested that this blue colour is scattered light originating from the microstructure consisting of nanoparticles. Moreover, the reflected light shows specific blue colour that originates with the specific microstructure in nano-scale. Since refractive index of the CaBBAT65 glass was 1.754 at 633

nm, there was a difference of refractive index, Δn, 0.8 or larger between the crystallized rutile and the surrounding glass matrix. Therefore, it is suggested that the nano-scale crystallization is the dominant factor for the transparency of the TiO_2 containing glass-ceramic even in such a large Δn situation. Note that such nanostructure was created using a conventional heat-treatment in an electric furnace. The nano-crystallization of TiO_2 is a kind of self-organization, and it is effective for making nano-scale particles in the matrix.

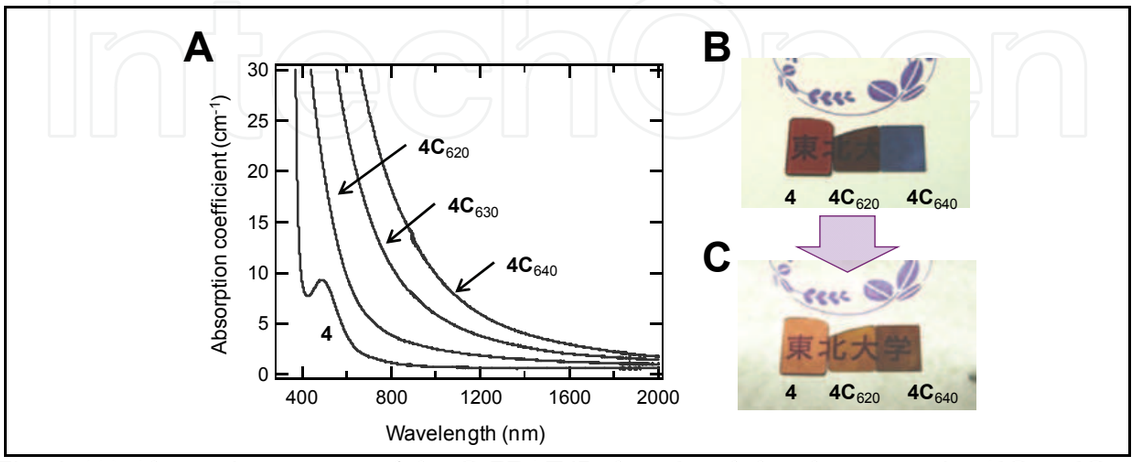

Fig. 6. (A) Absorption spectra of the CaBBAT65 glass **4** and the glass-ceramics (**4C**$_{620}$, **4C**$_{630}$, and **4C**$_{640}$). (B), (C) Photographs of several samples exposed by white light from front side (6(B)) and from the back side (6(C)).

Figure 7A shows XRD patterns of the CaBBAT65 glass-ceramics (**4C**$_{620}$, **4C**$_{630}$, and **4C**$_{640}$) together with that of the precursor glass (**4**). The glass-ceramics showed a mixture of the diffraction pattern of anatase (JCPDS No. 00-021-1272) and rutile. Since no diffraction peak assignable to other phases was observed, the obtained patterns show that TiO_2 crystallites were selectively formed as a single phase.

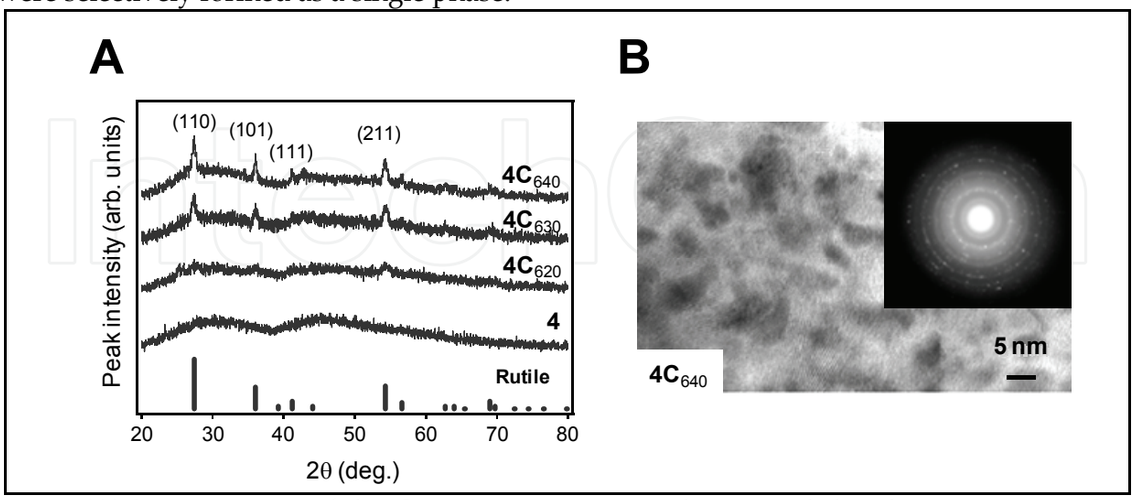

Fig. 7. (A) XRD patterns of the CaBBAT65 precursor glass **4**, and the glass-ceramics (**4C**$_{620}$, **4C**$_{630}$, and **4C**$_{640}$). (B) TEM image of the CaBBAT65 glass-ceramic (**4C**$_{640}$). Inset shows the electron diffraction pattern in which many satellites attributed to rutile are observed.

The average particle diameter measured by the Scherrer equation was 10~20 nm. Since no apparent change of the XRD pattern was observed after surface polishing of 500 μm, we can conclude that the bulk crystallization took place by the heat-treatment. Figure 7B shows the TEM image of the glass-ceramic (**4C**$_{640}$). Crystalline domains that have less than 10 nm diameter, which is comparable to the particle size of TiO_2 crystallites estimated by the XRD patterns, are observed. Inset shows the electron diffraction pattern of the glass-ceramic. The diffraction satellites attributable to rutile (110), (101), and (211) confirm the result of the XRD measurement. It is, therefore, suggested that the TiO_2 domains with small size distribution are the origin of the blue scattering from the glass matrix.

2.3 Sn-Doped CaBBAT Glass

As mentioned above, our group has prepared oxide semiconductor TiO_2-precipitated glass-ceramic for the first time in 2007. However, the CaBBAT precursor glass possesses a strong absorption band, which is correlated with the bismuth species, in the visible region. Since drastically compositional change was thought to be demerit for both a transparent glass and the glass-ceramic, addition of a small amount of other elements was considered to improve the transparency in the CaBBAT65 glass, and to maintain the selective crystallization behaviour of TiO_2 from the glass matrix.

Figure 8A shows the photograph of the CaBBAT65 glasses (**4**) and the SnO-containing CaBBAT glasses (**9**), (**10**), and (**11**), where the amounts of SnO were (**4**) 0, (**9**) 0.1, (**10**) 0.5, and (**11**) 1 mol%, respectively. The colours of the samples changed with increasing amount of SnO, and transparent glasses were obtained with SnO contents ranging from 0.1 to 1 mol%. On the other hand, precipitation of SnO_2 crystallites was observed in the sample containing 2 mol% of SnO, suggesting a limitation of SnO content. Figure 8B shows the absorption spectra of these glasses. The absorption coefficient in the visible region decreases drastically with addition of SnO and saturates with SnO of 0.5 mol%. The transmittance at 500 nm of the sample (**4**) was 10% whereas that of the glass (**10**) was about 70%, showing a clear improvement of the transparency by addition of SnO. If the change of valence of the Sn ion, from divalent to tetravalent in a glass melt or glass matrix, is responsible for the suppression of optical absorption, addition of oxides of multi-valent transition metals is expected to be also effective in improving the transparency. However, no improvement of transparency was observed in the CaBBAT glass containing such metal oxides as CeO_2, Cu_2O and Sb_2O_3 in which the valences of the metals are changeable. This indicates that the effect of SnO addition is not a simple redox-reaction. Since the absorption band depends on the chemical composition of a bismuth-containing glass, a structural change consisting of several ions should be considered for clarification of the mechanism.

In the Sn-doped CaBBAT glass, selective crystallization of TiO_2 was also attained by conventional heat-treatment. The Sn-doped CaBBAT glass-ceramic showed not only better transparency but also better photocatalytic property than the non-doped glass. Although the underlying mechanisms for the above effects remain to be clarified, the obtained results show that the SnO addition enhances both the transparency and the photocatalytic activity without any derogatory effect on the selective nature of TiO_2 precipitation.

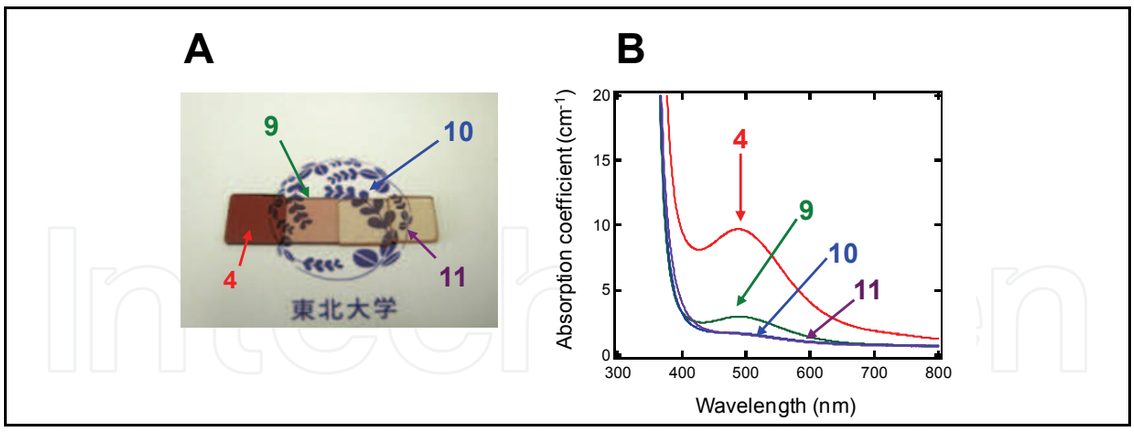

Fig. 8. (A) Photograph of the CaBBAT65 glasses with SnO-addition of (**4**) 0 mol%, (**9**) 0.1 mol%, (**10**) 0.5mol%, and (**11**) 1 mol%. (B) Absorption spectra of these CaBBAT65 glasses.

2.4 Bi-free TiO_2-Precipitated Glass-Ceramic

The CaBBAT glass, whether it contained SnO or not, contains a large amount of Bi_2O_3 as an essential component for TiO_2-glass-ceramic as well as transparent mother glass. Bi_2O_3 is, however, a hazardous material and there should be excluded from both environmental and industrial view point.

For fabrication of Bi-free TiO_2 glass-ceramics, we have focused on the bond dissociation energy of metal oxide in glass matrix (Sun, 1947). The concept is substitution several components, which have similar bond dissociation energy, for Bi_2O_3 in the CaBBAT glass. Since bond dissociation energy of Bi_2O_3 was not reported, we have calculated the single bond strength using the Born-Haber cyclic process (Lide & Kehiaian, 1994). The calculated value is shown as Eq. (1).

$$BiO1.5(s) \rightarrow Bi(g) + 1.5O(g) \quad + 868.2\ kJ/mol \tag{1}$$

Since the Bi unit in the oxide glass is reported as BiO_3 or BiO_6, we have estimated the single bond strength as 288.8 kJ/mol (BiO_3) and 142.3 kJ/mol (BiO_6), respectively. It follows that the former belongs to the intermediate group whereas the latter network modifier group. For substitution of Bi_2O_3, we have focused on ZnO that can belong to both intermediate (ZnO_2: bond dissociation energy 301.4 kJ/mol) or network modifier (ZnO_4: bond dissociation energy 150.7 kJ/mol) among several metal oxides. Since the bond dissociation energy of BiO_6 is similar to that of several alkaline earth oxides, RO, we have selected RO and ZnO for preparation of transparent Bi-free glass (R= Ca, Ba and Zn).

Table 2 shows the chemical composition of the obtained precursor glasses. Sample **4** depicts the previous CaBBAT65 glass whereas samples (**12**, **13**, **14**, and **15**) were transparent Bi-free glasses without devitrification during melt-quenching process. On the other hand, no homogeneous glass sample possessing composition of (**16**) or (**17**) was obtained. Therefore, it was found that neither direct substitution ZnO for Bi_2O_3 nor substitution without ZnO is effective for formation of transparent glass. The obtained results show that ZnO, which can play as an intermediate group or a network modifier group, has key for transparent homogeneous glass matrix.

No.	Chemical composition (mol%)						T_g (°C)
	TiO_2	ZnO	B_2O_3	CaO	BaO	Bi_2O_3	
4	20	0	65	5	0	10	570
12	20	10	65	5	10	0	580
13	20	10	65	0	15	0	589
14	20	20	65	5	0	0	587
15	20	25	65	0	0	0	608
16	20	10	65	5	0	0	–
17	20	0	65	25	0	0	–

Table 2. Chemical composition and T_gs of precursor glasses prepared with an alumina crucible. Homogeneous glasses possessing chemical composition of (**16**) and (**17**) were not obtained. (For easy comparison to the glass (**4**), the total amount of oxides exceeds 100 mol% in glasses (**12**) – (**17**).)

Figure 9A shows absorption spectra of the mother glasses: the CaBBAT65 glass (**4**), the SnO-doped CaBBAT65 glass (**10**), and the Bi-free glass (**12**). Figure 9B shows photograph of these glasses. The previous glasses were coloured (**4**, **10**) whereas the Bi-free glass (**12**) shows better transparency in the wavelength region. The result also confirms that Bi species are the origin of the absorption band around 500 nm as reported in several papers. Therefore, we can conclude that the substitution of Bi is effective for the improvement of transparency of the mother glass.

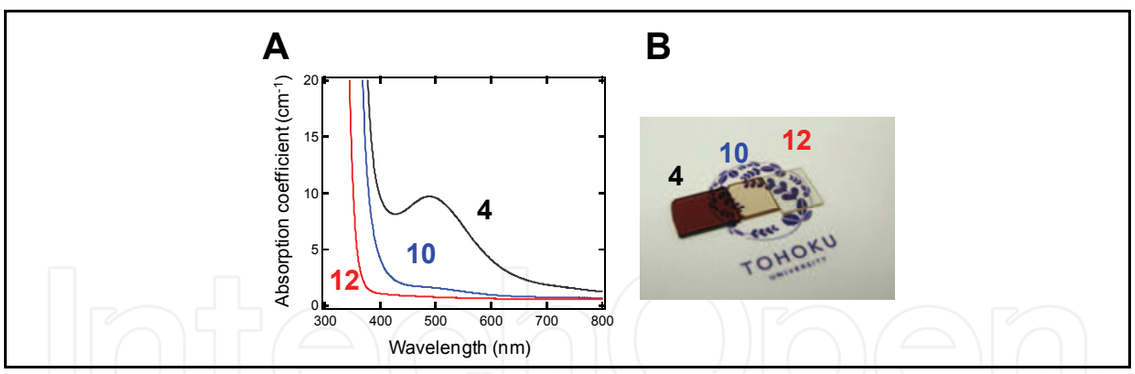

Fig. 9. (A) Absorption spectra of (**4**) the CaBBAT65 glass, (**10**) the SnO-doped CaBBAT65 glass, and (**12**) the Bi-free glass. (B) Photograph of these mother glasses.

Figure 10A shows the XRD patterns of the previous CaBBAT (**4**C_{630} and **10**C_{630}) and the Bi-free (**12**C_{630}) glass-ceramics together with photograph of these glasses. The JCPDS patterns of anatase and rutile are also shown in the figure for reference. The diffraction patterns of Bi-containing glass-ceramics (**4**C_{630} and **10**C_{630}) show precipitation of rutile whereas the pattern of the Bi-free glass-ceramic (**12**C_{630}) shows a mixture of anatase and rutile. We can estimate the average diameter of TiO_2 crystallites in the glass-ceramic (**12**C_{630}) as about 10 nm using the Scherrer equation. Note that the previous glass-ceramics (**4**C_{630} and **10**C_{630}) shows the blue colour, which is originated from the microstructure consisting of nano-particles, whereas the Bi-free glass-ceramic (**12**C_{630}) shows good transparency. The XRD

pattern and appearance of the glass-ceramic indicate that a TiO_2 nano-crystallization has been also attained without Bi_2O_3. Figure 10B shows the TEM image of the glass-ceramic (**12C**$_{630}$). The dashed circles show that the diameter of domains is several nanometres, which is comparable to the particle size of anatase crystallites estimated by the XRD patterns. Inset shows the electron diffraction pattern of the TiO_2 glass-ceramic at the circled region. The diffraction satellites attributable to anatase (101) confirm the result of the XRD measurement. These domains, therefore, are attributed to the anatase nano-crystallites in the glass matrix. It is also of interest that (101) diffraction of anatase is clearly observed in the Bi-free glass-ceramic (**12C**$_{630}$). Since anatase is metastable phase, we could observe no clear diffraction pattern of anatase in the Bi-containing CaBBAT glass-ceramics with various heat-treatment conditions. Therefore, we can conclude that the addition of ZnO improves the transparency of the TiO_2 glass-ceramics, and affects the crystallization of metastable phase.

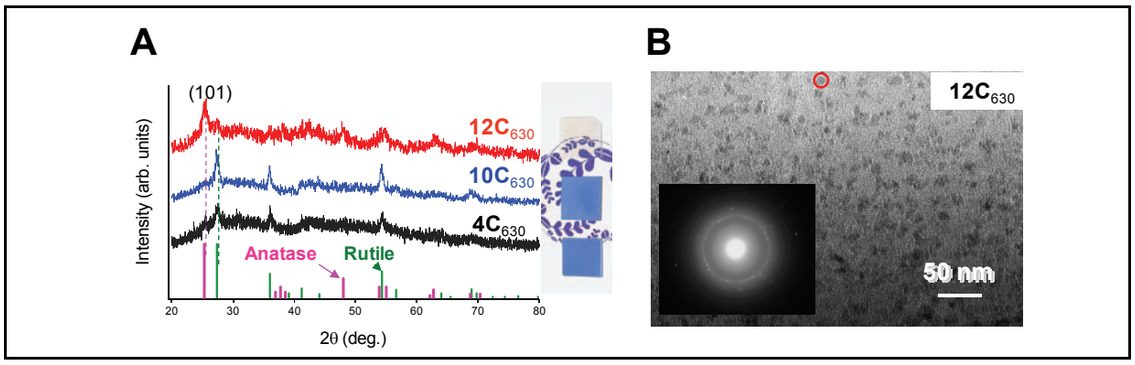

Fig. 10. (A) XRD patterns and photograph of TiO_2 glass-ceramics: the CaBBAT (**4C**$_{630}$), the SnO-doped CaBBAT (**10C**$_{630}$), and the Bi-free (**12C**$_{630}$) glass-ceramics. JCPDS patterns of anatase and rutile are also shown. (B) TEM image of the Bi-free glass-ceramic (**12C**$_{630}$). Inset shows electron diffraction pattern of the circled region.

Since the present approach for substitution of Bi_2O_3 is based on the bond dissociation energy, it can be said that the attempt is a kind of thermodynamically approach in homogeneous glass materials. We have hypothesized that Bi_2O_3 exists conjugated state of network modifier and intermediate. Although there is no clear evidence for coordination state of Bi_2O_3, our hypothesis is plausible, because (1) intermediate TiO_2 that possesses dissociation energy of 305.6 kJ/mol could not be substituted for ZnO, and (2) network modifier CaO makes no homogeneous glass without ZnO (see sample **17**). Therefore, ZnO, which can also play both roles, is effective for fabrication of Bi-free glass and the glass-ceramics. In the substitution, we have decided that amount of Bi cation should be equal to that of sum of other cations.

We examined the photocatalytic property of the TiO_2 glass-ceramics using a conventional decomposition reaction of methylene blue. Details of the measurement are shown in the paper (Masai et al. 2008). The decomposition reaction coefficient, k, of the previous glass-ceramic (**4C**$_{630}$) was 0.59 h^{-1} m^{-2}. On the other hand, k of the **12C**$_{630}$ glass-ceramics, in which anatase was crystallized, was 0.78 h^{-1} m^{-2}. If we consider the effective decomposition reaction rate per TiO_2, the rate of the previous glass-ceramic is 0.0295 h^{-1} m^{-2} mol^{-1} whereas that of the present glass-ceramic is 0.056 h^{-1} m^{-2} mol^{-1}. The obtained result shows that

precipitation of anatase is effective for high photocatalytic property of the glass-ceramics. The obtained result shows that precipitation of anatase is effective for high photocatalytic property of the glass-ceramics.
In summary, we have fabricated anatase precipitated glass-ceramics that possesses high transparency. The anatase nano-crystallites in the glass, confirmed by XRD and TEM measurements, show higher photocatalytic activity than the rutile nano-crystallites. It is also clarified that difference of precipitated TiO_2 phase is caused by the surrounding amorphous region. Our study has emphasized the potential of the transparent Bi-free glass-ceramic containing anatase nano-crystallites for transparent photocatalytic applications without any coating process. The result is a strong backup for fabrication of TiO_2 transparent glass-ceramics for photocatalytic application.

3. Glass-Ceramics Containing ZnO Nano-Crystallites

3.1 Background

ZnO is a kind of oxide semiconductors. As mentioned in many reports (Look, 2001, Özgür at al. 2005), semiconductor ZnO has attracted attention as a promising material for optoelectronic, optical, electronic, and photocatalytic devices. For examples, excitonic lasing that originates from the large exciton binding energy from ZnO thin film (Bagnall at al. 1998, Tang at al. 1999, Huang at al. 2001), luminescence from p-i-n ZnO junction (Tsukazaki et al., 2005), or green luminescence by oxygen vacancies in ZnO (Vanheusden et al., 1996) have been reported. On the other hand, using high refractive index of ZnO, random lasing from ZnO crystallites has been also reported (Cao et al., 2000). Although there have been many reports on the ZnO in thin film, powdered, or ceramic shape (Gupta, 1990), there is little report on the ZnO glass-ceramics that possesses both unique property of ZnO and good formability of glass material. Since Zn cation tends to form binary zinc crystallites with B_2O_3, SiO_2 during the crystallization process of glass matrix, it is difficult to obtain glass-ceramics with ZnO nano-crystallites. Recently, Pinckney has reported transparent glass-ceramics, in which ZnO nano-crystallites of 5-20 nm were selectively precipitated, by heat-treatment of SiO_2-Al_2O_3-ZnO-K_2O glass (Pinckney, 2006). The material was one of the few transparent glass-ceramics containing a semiconductor crystal phase. However, since amount of SiO_2 was 40-55 mol%, the melt temperature of the glass was relatively high (1575-1650°C), which is disadvantage for shaping process as well as crystallization process.
In this study, we have fabricated ZnO glass-ceramic based on borate glass. The CaO-B_2O_3-ZnO-Al_2O_3-K_2O-SiO_2 glass was prepared by conventional melt-quenching method with melt temperature at 1350°C, which was 200°C lower than the previous melt temperature. By investigation of chemical composition, we have found that Al_2O_3, alkali metal oxide and alkaline earth metal oxide are needed for obtaining transparent mother glass. On the other hand, precipitation of $Zn_3B_2O_6$ (Chen et al., 2006) or $KZn_4B_3O_9$ (Chen et al., 2005) was observed in glass-ceramics without SiO_2. According to the classification of oxide reported by Sun, SiO_2, Al_2O_3, and B_2O_3 belong to glass network former group that possess strong metal-oxygen bond whereas K_2O and CaO glass network modifier group that possess weak metaloxane bond. Since ZnO play intermediate group or network modifier group, it is suggested that ZnO can exist in the glass network in a diversified state. Considering the precipitation of ZnO phase after heat-treatment, we assume that ZnO disperses with weak bonding to main glass network.

3.2 CaO- B_2O_3-ZnO-Al_2O_3-K_2O (CaBZAK) Glass

For determination of chemical composition, we consulted the previous reports on TiO_2 glass-ceramics as mentioned above (Masai et al., 2007, 2008, 2009). Although we have investigated the crystallization behaviour of several glass systems, such as CaO-B_2O_3-Bi_2O_3-Al_2O_2-ZnO, CaO-B_2O_3-Al_2O_3-ZnO, CaO-B_2O_3-Al_2O_3-ZnO-SiO_2, crystallization of ZnO was hardly observed. Therefore, we firstly investigated the CaO-B_2O_3-ZnO-Al_2O_3-K_2O (CaBZAK) system for attainment of ZnO-precipitated glass-ceramics.

Glass samples were prepared by conventional melt-quenching method using alumina crucibles or platinum crucible. Table 3 shows the chemical compositions of the CaBZAK precursor glasses (**18**–**22**) together with their T_g values. Asterisks indicate that the corresponding glasses were prepared by alumina crucibles. Figure 11 shows XRD patterns of the 10CaO-40B_2O_3-40ZnO-Al_2O_3-10K_2O glass-ceramics. JCPDS pattern of ZnO (JCPDS No. 00-021-1272) was also shown. Heat-treatment of these glass-ceramics was performed at T_g +70~100 K for 3 h. It clearly shows that precipitated crystalline phase depended on the amount of Al_2O_3. Glass-ceramics with small amount of Al_2O_3 shows $KZn_4B_3O_9$ (**18C**$_{570}$) and α-$Zn_3B_2O_6$ (**19C**$_{550}$). On the other hand, ZnO was precipitated together with α-$Zn_3B_2O_6$ in the glass-ceramic containing over 10 mol% of Al_2O_3 (**20C**$_{595}$, **21C**$_{597}$, and **22C**$_{590}$,). Compared XRD pattern of glass-ceramic prepared with platinum crucible with that of glass-ceramic prepared with alumina crucible, the amount of Al_2O_3 eluted from crucible was estimated about 10~12 mol%. Compared ZnO-precipitated glass-ceramics with TiO_2-precipitated glass-ceramics, we have noticed that precipitation of oxide crystallites depends on the coordination state in glass matrix. In other words, even if oxide semiconductor was selectively precipitated from borate-based glasses, TiO_6 octahedra in glass cannot be directly substituted by ZnO_4 tetrahedra. The obtained XRD patterns show that Al_2O_3 strongly affects the crystallization behaviour of glass-ceramics. Since ZnO works as intermediate (ZnO_2: bond dissociation energy 301 kJ/mol) or network modifier (ZnO_4: bond dissociation energy 151 kJ/mol), it is suggested that additional Al_2O_3, which can work as a network former, affects coordination state of ZnO into a network modifier. Note that Zinc takes 4-coordination state in precipitated crystallites, such as $KZn_4B_3O_9$, α-$Zn_3B_2O_6$, or ZnO.

No.	Chemical composition (mol%)						T_g
	CaO	K_2O	SiO_2	B_2O_3	ZnO	Al_2O_3	(°C)
18	10	10	0	40	40	0	483
19	10	10	0	40	40	5	485
20	10	10	0	40	40	10	492
21	10	10	0	40	40	12	503
22	10	10	0	40	40	*	495
23	10	10	10	25	45	*	525
24	10	10	20	20	40	*	544
25	5	5	15	25	50	*	542
26	10	10	5	30	45	*	507
27	10	10	20	25	35	*	526

Table 3. Chemical composition and T_gs of precursor glasses for precipitation of ZnO. Asterisks indicate that the corresponding glasses were prepared by alumina crucibles.

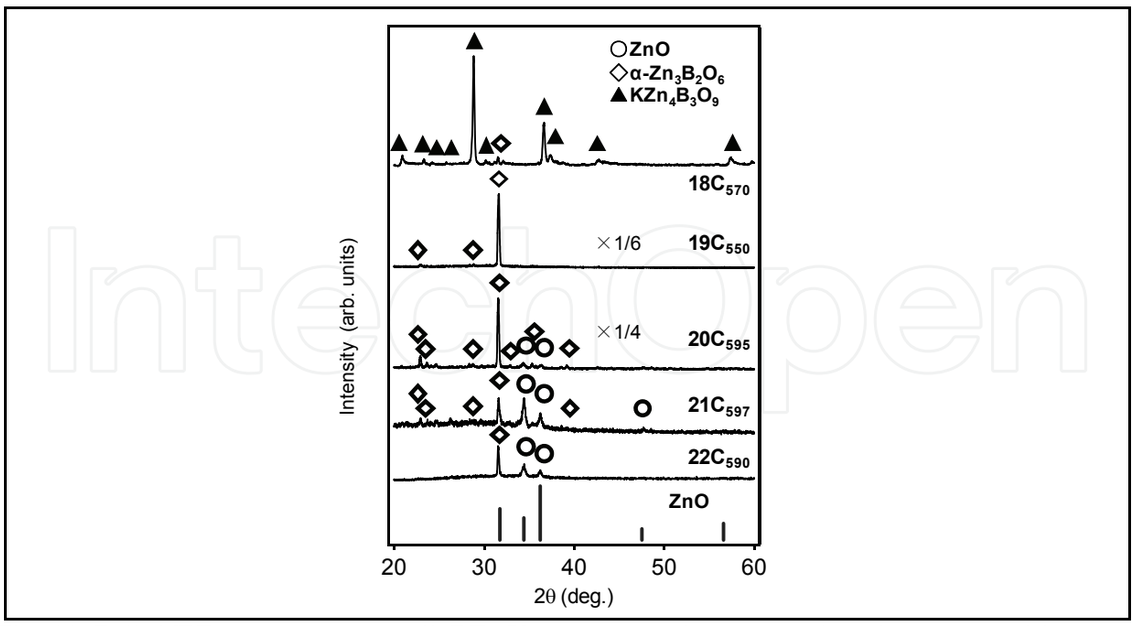

Fig. 11. Bulk XRD patterns of the CaBZAK glass-ceramics whose chemical compositions are listed in Table 3. Diffraction pattern of ZnO (JCPDS No. 00-021-1272) is also shown.

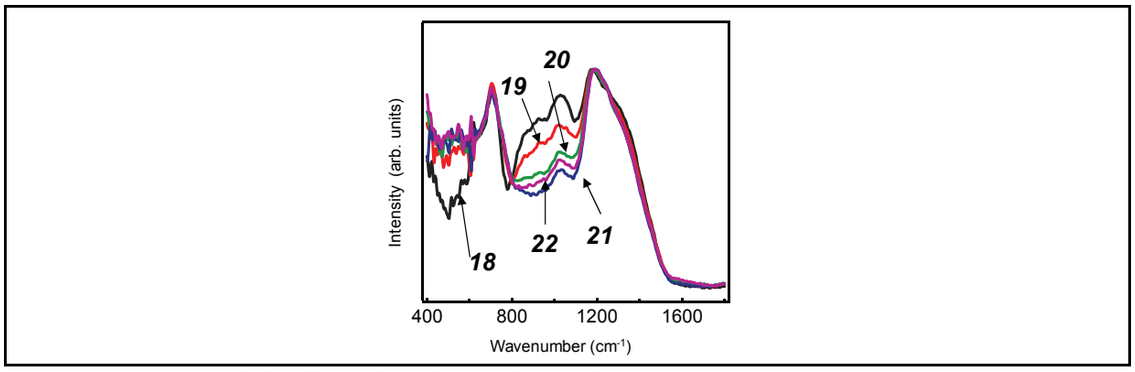

Fig. 12. IR spectra of the CaBZAK glasses (**18**–**22**)

Figure 12 shows IR spectra of the 10CaO-40B_2O_3-40ZnO-Al_2O_3-10K_2O glasses (**18**–**22**). Spectra are normalized using band around 1160 cm^{-1}, which belongs to the B–O–B vibration mode of the trigonal BO_3 unit. Band at 400~600 is attributed to ZnO_4 tetrahedra whereas the band around 700 cm^{-1} is assigned to the bending vibration of the B–O–B linkage. Band attributed to ZnO_4 increased by addition of Al_2O_3. On the other hand, signals from 800 to 1200 cm^{-1} that are assigned to tetrahedral BO_4 unit decrease with increasing amount of Al_2O_3. Observed band attributable to B-O-B was shifted to longer wavelength with increasing amount of Al_2O_3. The IR spectra of the glasses show that glass network has changed after addition of Al_2O_3. Since Al_2O_3 can make glass network, trigonal BO_3 unit that possess weaker network than tetrahedral BO_4 unit increases by addition of Al_2O_3 as a counterpart. Concurrently, band attributed to ZnO_4, which is similar structure of ZnO crystal, increased. Thus, it is speculated that isolated ZnO_4 was formed in glass matrix after addition of Al_2O_3. On the other hand, observed band around 1170 cm^{-1} attributable to B-O-B was shifted to

longer wavelength with increasing amount of Al_2O_3. Since the stretching force constant of Zn–O bond is lower than that of B–O, the frequency of Zn–O–B might appear at lower region. Thus, it is suggested that observed shift by addition of Al_2O_3 reflects the change from Zn-O-B bond to B-O-B bond in the glass. The decrease of number of Zn-O-B bond will affect the crystallization behaviour with precipitation of ZnO. That is a plausible mechanism for precipitation of ZnO instead of α-$Zn_3B_2O_6$.

3.3 CaO-B_2O_3-ZnO-Al_2O_3-K_2O-SiO_2 (CaBZAKS) Glass

Although we found that Al_2O_3 affected the crystallization behaviour of glass-ceramics, there was a limit of Al_2O_3 content for vitrification of glass. To attain selective crystallization of ZnO after heat-treatment, precipitation of α-$Zn_3B_2O_6$ should be prevented. Since homogeneous transparent glass was not obtained by addition over 12 mol% of Al_2O_3, we used partially substitution of network former from B_2O_3 to SiO_2. Here, we called the CaO-B_2O_3-ZnO-Al_2O_3-K_2O-SiO_2 glass system as CaBZAKS. Figure 13A shows photograph of the CaBZAKS mother glass (**23**) and the glass-ceramics (**23C**$_{610}$). The obtained glass-ceramics showed transparency despite of large difference of refractive index between ZnO and surrounding glass matrix. Figure 13B shows TEM image of the CaBZAKS glass-ceramics (**23C**$_{610}$). Rod-like ZnO crystallites were precipitated from the surface of the sample, and the crystal size was less than 1 μm. It is noted that the obtained glass-ceramic shows transparency despite a difference of refractive index, Δn, 0.4 between the precipitated ZnO (~2.0) and surrounding glass matrix (1.59~1.63). Figure 13C depicts XRD patterns of several CaBZAKS glass-ceramics (**23C**$_{610}$, **24C**$_{660}$, **25C**$_{660}$, **26C**$_{610}$, and **27C**$_{620}$) together with diffraction pattern of ZnO. Although diffraction intensities of each sample are different from the JCPDS pattern, we have confirmed that ZnO was selectively crystallized in all cases.

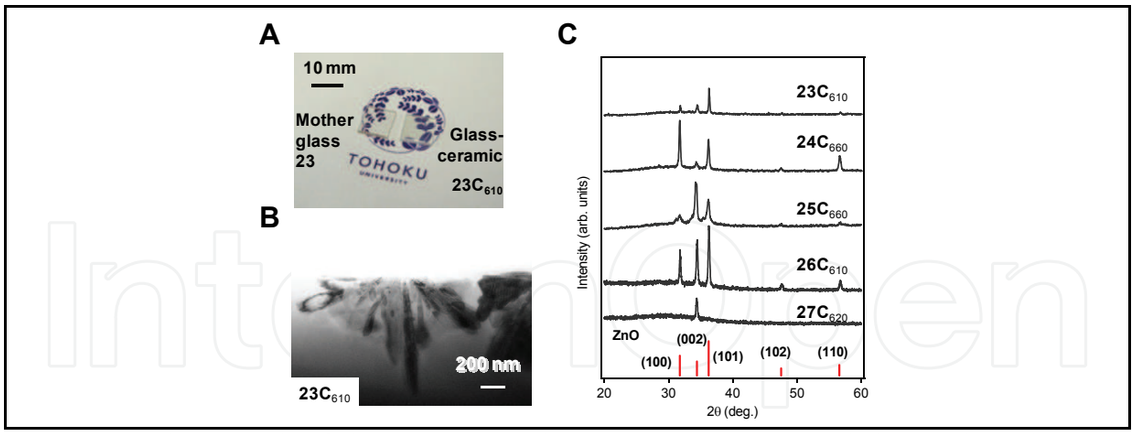

Fig. 13. (A) Photograph of the CaBZAKS glass-ceramic (**23C**$_{610}$) and the mother glass (**23**). (B) TEM image of the CaBZAKS glass-ceramic (**23C**$_{610}$). (C) XRD patterns of several CaBZAKS glass-ceramics together with JCDPS pattern of ZnO.

We have found the emission property of the ZnO precipitated glass-ceramics similar to that of ZnO single crystal. Figure 14 shows photoluminescence spectra of the ZnO glass-ceramics (**23C**$_{600}$, **23C**$_{610}$, and **23C**$_{640}$) and the mother glass (**23**). The spectra were measured at room temperature using a He-Cd laser as a light source. The glass-ceramic **23C**$_{640}$ was opaque because of scattering by surface crystallized ZnO. The glass-ceramic shows emission

at 3.28 eV, which is assigned to free exciton emission of ZnO. The emission spectrum of ZnO glass-ceramic is similar to that of ZnO single crystal. It indicates that crystal growth of ZnO occurred enough to show the exciton emission. We can find several characteristics in the obtained emission spectra of the ZnO glass-ceramics and the mother glass. The mother glass roughly consists of two broad bands at 1.4~2.6 eV. The emission at 1.4-2.6 eV is attributable to oxygen vacancies of ZnO (Vanheusden et al., 1996, Djurisic et al., 2007). On the other hand, the intensity of emission at 3.28 eV, which is assigned to free exciton emission of ZnO, clearly observed in the glass-ceramic. Since the thickness of crystallized region in the ZnO-precipitated glass-ceramics was about 1 μm from the surface, the volume percentage of ZnO crystals shown in Fig. 14 was less than 1 volume %. The results indicate that emission from the glass-ceramics depends on the state of precipitated ZnO crystallites, and that unique property of ZnO can be equipped in the glass-ceramics by optimized crystallization process (Masai et al., 2009).

In summary, we have obtained transparent ZnO-precipitated glass-ceramic. The ZnO nano-crystallites that were precipitated at the surface of the glass showed both broad emission and free exciton emission. The observed emission depends on the precipitated state of ZnO in the glass matrix, and has great potential for optical devices. The large Δn between ZnO crystallites and the surrounding glass matrix warrants the localization of photon, which is also attractive as optical ceramic devices. Note that crystallization behaviour, such as orientation of precipitated phase, or size of crystallites, in the glass matrix can be controlled. The present ZnO glass-ceramics could be an attractive functional material using the advantage of the amorphous glass material, which is quite different from conventional ZnO material.

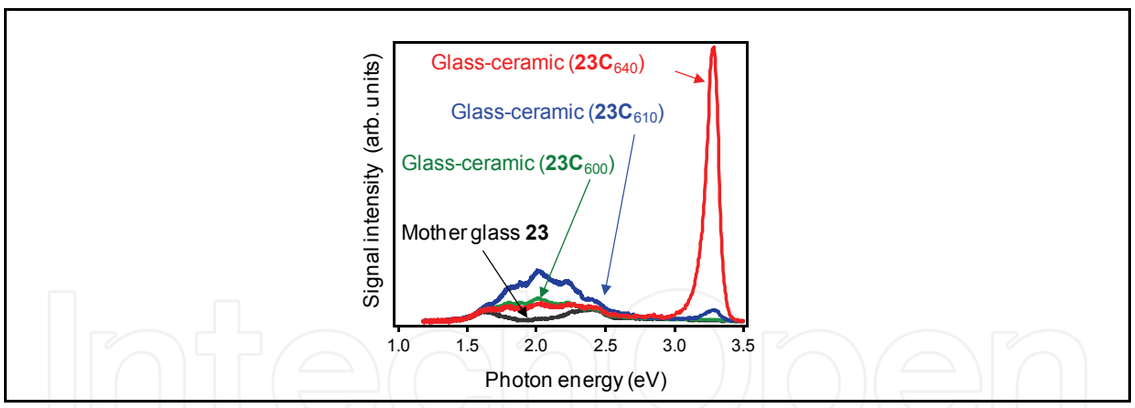

Fig. 14. Photoluminescence spectra of ZnO glass-ceramics (**23C**$_{600}$, **23C**$_{610}$, and **23C**$_{640}$) and the mother glass (**23**) using a He-Cd laser as a light source.

4. Current and Future Trends in Glass-Ceramics

Our results above-mentioned were achieved by examination of both the chemical composition and the crystallization process by traditional heat-treatment using electric furnace. Since the crystallization of glass by conventional heat-treatment is based on the self-organization of crystal above the T_g, the crystallization technique is favourable for industrial process in which simplified process and mass production are required. However, the method is not suitable for microstructuring of glass-ceramics consisting of locally

crystallized region at less than micrometres. Recently, there have been many reports on another process for space selective crystallization: laser-induced crystallization. The crystallization has been attained by several kinds of lasers, such as ultra-fast (e.g. femto-second) pulsed laser (Kondo et al., 1998, Yonesaki et al., 2005), nano-second pulsed laser (Fujiwara et al., 2002, Mizuno et al., 2006, Masai et al., 2008), or continuous wave (CW) laser (Sato et al., 2001, Honma et al., 2003 & 2006). Laser irradiation can induce a geometrically selective structural change, which is quite different from uniform bulk structural change caused by a conventional heating process using a furnace. If laser irradiation can induce a change of refractive index or crystallization in a glass matrix, such laser-induced structures provide unique properties without temporal decay. However, there is a difference between a femto-second laser and a nano-pulsed laser and a CW laser from the view point of the mechanism of laser-induced change in the irradiated material. The former can induce local changes with little thermal effect whereas the latter two actively exploits the thermal effect for laser-induced change. If we use the crystallization of oxides for functionalization of glass, control of the thermal process should be necessary. Irradiation of glass materials with a laser having a thermal effect, therefore, is thought to be effective in preparing functional devices using controllable crystallization behaviour. In using a thermal effect for a laser-induced structural change, the change depends on temperature and holding duration above the T_g. If we can control the temperature and a holding duration of the temperature, we can control the formation of crystallite nuclei and the growth of crystallites the respective, which is of great importance in creating tailored local structures. For example, nano-second pulsed laser irradiation can induce surface structural change of glass, in which nanostructure at tens or hundreds of nanometres are formed (see Fig. 15A & 15B). On the other hand, irradiation of not only a femto-second pulsed laser but also a CW laser (Fig. 15C) can induce crystallization inside the matrix. Such glass-ceramics are expected to be functional devices possessing lightwave controllability that is not inherent property of amorphous glasses.

By using the laser-irradiation technique, it is expected that above-mentioned oxide semiconductor-precipitated glass-ceramics will show the novel development. Designed nanostructure at the surface of glass-ceramic is effective not only for photocatalyst that requires large surface area but also light controllable device, such as photonic crystal, using the high refractive index. Control of orientation of precipitated crystallites at the surface is also of interest for applied science. On the other hand, internal structural change will work as an integrated circuit or an origin for emission centre.

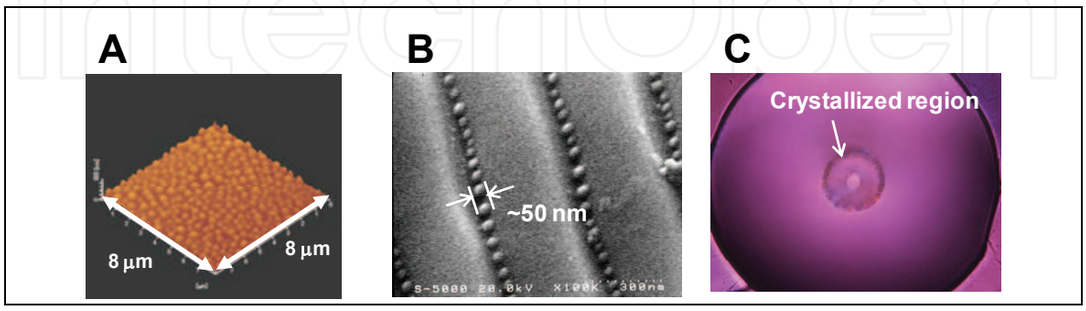

Fig. 15. Various laser-induced structural changes: AFM and SEM images of structural change of glass induced by a pulsed laser with (A) uniform and (B) interfering irradiations. (C) Photograph of the internal crystallization in a multi-structured fibre by irradiation of CW laser (reported by Ohara et al., 2009).

However, besides examination of crystallization of glass by laser-irradiation technique or conventional heat-treatment, deeper understanding of glass material itself is of necessity. The glass-ceramics can open up an application field for functional glass-based device, and therefore, the design and control of nanostructure in these materials will be of great importance.

5. Conclusion

In the present study, we have demonstrated fabrication of glass-ceramics containing two oxide semiconductors, TiO_2 and ZnO. It is notable that selective crystallization of these crystallites was successfully attained by examination of both the chemical composition of glass and the heat-treatment procedure. Moreover, the obtained glass-ceramics possessed transparency despite of large difference of refractive index. Our results mentioned were demonstrated by conventional heat-treatment using an electric furnace that is favourable for industrial process. As mentioned in the introduction and the last sections, crystallization of glass can take wide diversity of structure and the related physical property. The investigation of the novel property using glass-ceramics will be continued now and for the future.

6. References

Bagnall, D. M.; Chen, Y. F.; Zhu, Z.; Yao, T.; Shen, M. Y. & Goto, T. (1998). High temperature excitonic stimulated emission from ZnO epitaxial layers. *Appl. Phys. Lett.* 73, 8, 1038-1040, 0003-6951.

Beall, G. H. & Pinckney, L. R. (1999). Nanophase glass-ceramics. *J. Am. Ceram. Soc.* 82, 1, 5-16, 0002-7820.

Brydges, W. T. III & Smith, D. W. *US Patent* 3948669 (1976).

Cao, H.; Xu, J. Y.; Seelig, E. W. & Chang, R. P. H. (2000). Microlaser made of disordered media. *Appl. Phys. Lett.* 76, 21, 2997-2999, 0003-6951.

Ling, Y.; CaO, H.; Burin A. L.;Ratner, M. A.; Liu, X. & Chang, R. P. H. (2001). Investigation of random lasers with resonant feedback. *Phys. Rev. A* 64, 6, 063808, 1050-2947.

Chen, X.; Xue, H.; Chang, X.; Zhang, L.; Zhao, Y.; Zuo, J.; Zang, H. & Xiao, W. (2006). Syntheses and crystal structures of the alpha- and beta-forms of zinc orthoborate, $Zn_3B_2O_6$. *J. Alloy. Compd*, 425, 1-2, 96-100, 0925-8388.

Chen, D.-G.; Cheng, W.-D.; Wu, D.-S.; Zhang, H.; Zhang, Y.-C.; Gong, Y.-J. & Kan, Z.-G. (2005). Syntheses, band structures and optical properties of $Zn_3B_2O_6$ and $KZn_4B_3O_9$. *Solid State Sci*, 7, 2, 179-188, 1293-2558.

Djurisic, A. B.; Leung, Y. H.; Tam, K. H.; Hsu, Y. F.; Ding, L.; Ge, W. K.; Zhong, Y. C.; Wong, K. S.; Tam, H. L.; Cheah, K. W.; Kwok, W. M. & Phillips, D. L. (2007). Defect emissions in ZnO nanostructures. *Nanotechnology*, 18, 9, 095702, 0957-4484.

Fujishima, A. & Honda, K. (1972). Electrochemical photolysis of water at a semiconductor electrode. *Nature*, 238, 5358, 37-38, 0028-0836.

Fujiwara, T.; Ogawa, R.; Takahashi, Y.; Benino, Y. & Komatsu, T. (2002). Laser-induced photonic periodic structure in tellurite based glass ceramics. *Phys. Chem. Glasses*, 43C, 213-216, 0031-9090.

Gupta, T. K. (1990). Application of Zinc-oxide varistors. *J. Am. Ceram. Soc.* 73, 7, 1817-1840, 0002-7820.

Honma, T.; Benino, Y.; Fujiwara, T. & Komatsu, T. (2006). Transition metal atom heat processing for writing of crystal lines in glass. *Appl. Phys. Lett.* 88, 23, 231105, 0003-6951.

Honma, T.; Benino, Y.; Fujiwara, T.; Komatsu, T. & Sato, R. (2003). Technique for writing of nonlinear optical single-crystal lines in glass. *Appl. Phys. Lett.* 83, 14, 2796-2798, 003-6951.

Hosono, H.; Sakai, Y.; Fasano, M. & Abe, Y. (1990). Preparation of monolithic porous titania silica ceramics. *J. Am. Ceram. Soc.* 73, 8, 2536-2538, 0002-7820.

Huang, M. H.; Mao, S.; Feick, H.; Yan, H.; Wu, Y.; Kind, H.; Weber, E.; Russo, R. & Yang, P. (2001). Room-temperature ultraviolet nanowire nanolasers. *Science* 292, 5523, 1897-1899, 0036-8075.

Kato, K.; Fu, D.; Suzuki, K.; Tanaka, K.; Nishizawa, K. & Miki, T. (2004). High piezoelectric response in polar-axis-oriented $CaBi_4Ti_4O_{15}$ ferroelectric thin films. *Appl. Phys. Lett.* 84, 19, 3771-3773, 0003-6951.

Khonthon, S.; Morimoto, S.; Arai, Y. & Ohishi, Y. (2007). Luminescence characteristics of Te- and Bi-doped glasses and glass-ceramics. *J. Ceram. Soc. Jpn*, 115, 1340, 259-263, 0914-5400.

Kondo, Y.; Suzuki, T.; Inouye, H.; Miura, K.; Mitsuyu, T. & Hirao, K. (1998). Three-dimensional microscopic crystallization in photosensitive glass by femtosecond laser pulses at nonresonant wavelength. *Jpn. J. Appl. Phys.* 37, 1AB, L94-L96, 0021-4922.

Lawandy, N. M.; Balachandran, R. M.; Gomes, A. S. L. & Sauvain, E. (1994). Laser action in strongly scattering media. *Nature* 368, 6470, 436-438, 0028-0836.

Lide, D. R. & Kehiaian, H. V. (1994). *CRC handbook of thermophysical & thermochemical data*, CRC Press, 0849301971, Tokyo.

Look, D. C. (2001). Recent advances in ZnO materials and devices. *Mater. Sci. Engineer. B* 80, 1-3, 383-387, 0921-5107.

Masai, H.; Fujiwara, T.; Benino, Y. & Komatsu, T. (2006). Large second-order optical nonlinearity in $30BaO\text{-}15TiO_2\text{-}55GeO_2$ surface crystallized glass with strong orientation. *J. Appl. Phys.* 100, 2, 023526, 0021-8979.

Masai, H.; Fujiwara, T. & Mori, H. (2007). Fabrication of TiO_2 nano-crystallized glass, *Appl. Phys. Lett.* 90, 8, 081907, 0003-6951.

Masai, H.; Fujiwara, T. & Mori, H. (2008). Effect of SnO addition on optical absorption of bismuth borate glass and photocatalytic property of the crystallized glass. *Appl. Phys. Lett.* 92, 14, 141902, 0003-6951.

Masai, H.; Mizuno, S.; Fujiwara, T.; Mori, H. & Komatsu, T. (2008). Fabrication of metal nanocluster and nanoparticles in the $CaO\text{-}Bi_2O_3\text{-}B_2O_3\text{-}Al_2O_3\text{-}TiO_2$ glass by irradiation of XeCl pulsed laser. *Opt. Express*, 16, 4, 2614-2620, 1094-4087.

Masai, H.; Takahashi, Y.; Fujiwara, T.; Suzuki, T. & Ohishi Y. (2009). Correlation between NIR emission and bismuth radical species of Bi_2O_3-containing aluminoborate glass. *J. Appl. Phys.* 106, 10, 103523, 0021-8979.

Masai, H.; Toda, T.; Takahashi, Y. & Fujiwara, T. (2009). Fabrication of anatase precipitated glass-ceramics possessing high transparency. *Appl. Phys. Lett.* 94, 15, 151910, 0003-6951.

Masai, H.; Toda, T.; Ueno, T.; Takahashi, Y. & Fujiwara, T. (2009). ZnO glass-ceramics: An alternative way to produce semiconductor materials. *Appl. Phys. Lett.* 94, 15, 151908, 0003-6951.

McMillan, P. W. (1979). *Glass ceramics*, Academic Prss, 0124856608, London.

Mizuno, S.; Fujiwara, T.; Benino, Y. & Komatsu, T. (2006). Novel technique for fabrication of nanoparticle structures in $KNbO_3$-TeO_2 glass for photonic integrated circuits. *Jpn. J. Appl. Phys.* 45, 8A, 6121-6125, 0021-4922.

Murata, T. & Mouri, T. (2007). Matrix effect on absorption and infrared fluorescence properties of Bi ions in oxide glasses. *J. Non-Cryst. Solids* 353, 24-25, 2403-2407, 0022-3093.

Ohara, S.; Masai, H.; Takahashi, Y.; Fujiwara, T.; Kondo, Y. & Sugimoto, N. (2009). Space-selectively crystallized fiber with second-order optical nonlinearity for variable optical attenuation Opt. Lett. 34, 7, 1027-1029, 0146-9592.

O'Regan, B. & Gratzel, M. (1991). A Low-cost, high-efficiency solar-cell based on dye-sensitized colloidal TiO_2 films. *Nature* 353, 6346, 737-740, 0028-0836.

Özgür, Ü.; Alivov, Y. I. ; Liu, C.; Take, A.; Reshchikov, M. A.; Doğan, S.; Avrutin, V.; Cho, S.-J. & Morkoç, H. (2005). A comprehensive review of ZnO materials and devices. *J. Appl. Phys.* 98, 4, 041301, 0021-8979.

Pinckney, L. R. (2006). Transparent glass-ceramics based on ZnO crystals. *Phys. Chem. Glass: Eur. J. Glass Sci. Technol. B* 47, 2, 127-130. 0031-9090.

Sato, R.; Benino, Y.; Fujiwara, T. & Komatsu, T. (2001). YAG laser-induced crystalline dot patterning in samarium tellurite glasses. *J. Non-Cryst. Solids* 289, 1-3, 228-232, 0022-3093.

Strnad, Z. (1986). *Glass-ceramic materials*, Elesevier, 0444995242, Amsterdam.

Sun, K. H. (1947). Fundamental condition of glass formation. *J. Am. Ceram. Soc.* 30, 9, 277-281, 0002-7820.

Takahashi, Y.; Benino, Y.; Fujiwara, T. & Komatsu, T. (2001). Second harmonic generation in transparent surface crystallized glasses with stillwellite-type $LaBGeO_5$. *J. Appl. Phys.* 89, 10, 5282-5287, 0021-8979.

Takahashi, Y.; Benino, Y.; Fujiwara, T. & Komatsu, T. (2004). Large second-order optical nonlinearities of fresnoite-type crystals in transparent surface-crystallized glasses. *J. Appl. Phys.* 95, 7, 3503-3508, 0021-8979.

Tang, Z. K.; Wong, G. K.; Yu, P.; Kawasaki, M.; Ohtomo, A.; Koinuma, H. & Segawa Y. (1998). Room-temperature ultraviolet laser emission from self-assembled ZnO microcrystallite thin films. *Appl. Phys. Lett.* 72, 25, 3270-3272, 0003-6951.

Tsukazaki, A.; Ohtomo, A.; Onuma, T.; Ohtani, M.; Makino, T.; Sumiya, M.; Ohtani, K.; Chichibu, S. F.; Fuke, S.; Segawa, Y.; Ohno, H.; Koinuma, H. & Kawasaki, M. (2005). Repeated temperature modulation epitaxy for p-type doping and light-emitting diode based on ZnO. *Nature Materials* 4, 1, 42-46, 1476-1122.

Vanheusden, K.; Seager, C.H.; Warren W.L.; Tallant, D. R. & Voigt, J. A. (1996). Correlation between photoluminescence and oxygen vacancies in ZnO phosphors. *Appl. Phys. Lett.* 68, 3, 403-405, 0003-6951.

Yeung, K. S. & Lam, Y. W. (1983). A simple chemical vapor-deposition method for depositing thin TiO_2 films. *Thin Solid Films*, 109, 2, 169-178, 0040-6090.

Yonesaki, Y.; Miura, K.; Araki, R.; Fujita, K. & Hirao, K. (2005). Space-selective precipitation of non-linear optical crystals inside silicate glasses using near-infrared femtosecond laser. J. Non-Cryst. Solids 351, 10-11, 885-892, 0022-3093.

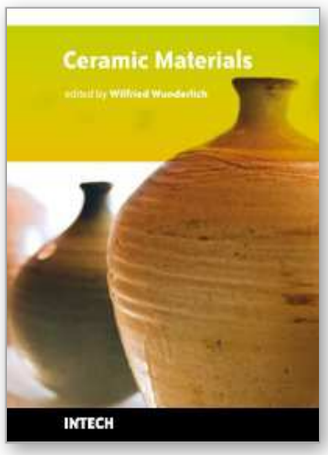

Ceramic Materials

Edited by Wilfried Wunderlich

ISBN 978-953-307-145-9
Hard cover, 228 pages
Publisher Sciyo
Published online 28, September, 2010
Published in print edition September, 2010

This is the first book of a series of forthcoming publications on this field by this publisher. The reader can enjoy both a classical printed version on demand for a small charge, as well as the online version free for download. Your citation decides about the acceptance, distribution, and impact of this piece of knowledge. Please enjoy reading and may this book help promote the progress in ceramic development for better life on earth.

How to reference

In order to correctly reference this scholarly work, feel free to copy and paste the following:

Hirokazu Masai, Yoshihiro Takahashi and Takumi Fujiwara (2010). Glass-Ceramics Containing Nano-Crystallites of Oxide Semiconductor, Ceramic Materials, Wilfried Wunderlich (Ed.), ISBN: 978-953-307-145-9, InTech, Available from: http://www.intechopen.com/books/ceramic-materials/glass-ceramics-containing-nano-crystallites-of-oxide-semiconductor

INTECH
open science | open minds

InTech Europe
University Campus STeP Ri
Slavka Krautzeka 83/A
51000 Rijeka, Croatia
Phone: +385 (51) 770 447
Fax: +385 (51) 686 166
www.intechopen.com

InTech China
Unit 405, Office Block, Hotel Equatorial Shanghai
No.65, Yan An Road (West), Shanghai, 200040, China
中国上海市延安西路65号上海国际贵都大饭店办公楼405单元
Phone: +86-21-62489820
Fax: +86-21-62489821

IntechOpen